

Monte Carlo simulations and n-p differential scattering data measured with Proton Recoil Telescopes

N. Terranova^{1,2,*}, O. Aberle³, V. Alcayne⁴, S. Amaducci^{5,6}, J. Andrzejewski⁷, L. Audouin⁸, V. Babiano-Suarez⁹, M. Bacak^{3,10,11}, M. Barbagallo^{3,12}, S. Bennett¹³, E. Berthoumieux¹¹, D. Bosnar¹⁴, A. S. Brown¹⁵, M. Busso^{16,17}, M. Caamaño¹⁸, L. Caballero⁹, M. Calviani³, F. Calviño¹⁹, D. Cano-Ott⁴, A. Casanovas¹⁹, F. Cerutti³, E. Chiaveri^{13,20,3}, N. Colonna¹², G. P. Cortés¹⁹, M. A. Cortés-Giraldo²⁰, L. Cosentino⁵, S. Cristallo^{16,21}, L. A. Damone^{12,22}, P. J. Davies¹³, M. Diakaki²³, M. Dietz²⁴, C. Domingo-Pardo⁹, R. Dressler²⁵, Q. Ducasse²⁶, E. Dupont¹¹, I. Durán¹⁸, Z. Eleme²⁷, B. Fernández-Domínguez¹⁸, A. Ferrari³, I. Ferro-Gonçalves²⁸, P. Finocchiaro⁵, V. Furman²⁹, R. Garg²⁴, A. Gawlik⁷, S. Gilardoni³, K. Göbel³⁰, E. González-Romero⁴, C. Guerrero²⁰, F. Gunsing¹¹, S. Heinitz²⁵, J. Heyse³¹, D. G. Jenkins¹⁵, E. Jericha¹⁰, U. Jiri²⁵, A. Junghans³², Y. Kadi³, F. Käppeler³³, A. Kimura³⁴, I. Knapová³⁵, M. Kokkoris²³, Y. Kopatch²⁹, M. Krtička³⁵, D. Kurtulgil³⁰, I. Ladarescu⁹, C. Lederer-Woods²⁴, J. Lerendegui-Marco²⁰, S.-J. Lonsdale²⁴, D. Macina³, A. Manna^{36,37}, T. Martínez⁴, A. Masi³, C. Massimi^{36,37}, P. F. Mastinu³⁸, M. Mastroianni^{3,13}, E. Mauger²⁵, A. Mazzone^{12,39}, E. Mendoza⁴, A. Mengoni^{36,40}, V. Michalopoulou^{3,23}, P. M. Milazzo⁴¹, M. A. Millán-Callado²⁰, F. Mingrone³, J. Moreno-Soto¹¹, A. Musumarra^{5,6}, A. Negret⁴², F. Ogállar⁴³, A. Oprea⁴², N. Patronis²⁷, A. Pavlik⁴⁴, J. Perkowski⁷, C. Petrone⁴², L. Piersanti^{16,21}, E. Pirovano²⁶, I. Porras⁴³, J. Praena⁴³, J. M. Quesada²⁰, D. Ramos Doval⁸, R. Reifarth³⁰, D. Rochman²⁵, C. Rubbia³, M. Sabaté-Gilarte^{20,3}, A. Saxena⁴⁵, P. Schillebeeckx³¹, D. Schumann²⁵, A. Sekhar¹³, A. G. Smith¹³, N. Sosnin¹³, P. Sprung²⁵, A. Stamatopoulos²³, G. Tagliente¹², J. L. Tain⁹, A. E. Tarifeño-Saldivia¹⁹, L. Tassan-Got^{3,23,8}, B. Thomas³⁰, P. Torres-Sánchez⁴³, A. Tsinganis³, S. Ullrich^{3,32}, S. Valenta³⁵, G. Vannini^{36,37}, V. Variale¹², P. Vaz²⁸, A. Ventura², D. Vescovi^{16,46}, V. Vlachoudis³, R. Vlastou²³, A. Wallner⁴⁷, P. J. Woods²⁴, T. J. Wright¹³, and P. Žugec¹⁴

¹Agenzia nazionale per le nuove tecnologie, l'energia e lo sviluppo economico sostenibile (ENEA), Frascati, Italy

²Istituto Nazionale di Fisica Nucleare, CNAF, Bologna, Italy

³European Organization for Nuclear Research (CERN), Switzerland

⁴Centro de Investigaciones Energéticas Medioambientales y Tecnológicas (CIEMAT), Spain

⁵INFN Laboratori Nazionali del Sud, Catania, Italy

⁶Dipartimento di Fisica e Astronomia, Università di Catania, Italy

⁷University of Lodz, Poland

⁸IPN, CNRS-IN2P3, Univ. Paris-Sud, Université Paris-Saclay, F-91406 Orsay Cedex, France

⁹Instituto de Física Corpuscular, CSIC - Universidad de Valencia, Spain

¹⁰Technische Universität Wien, Austria

¹¹CEA Saclay, Irfu, Université Paris-Saclay, Gif-sur-Yvette, France

¹²Istituto Nazionale di Fisica Nucleare, Bari, Italy

¹³University of Manchester, United Kingdom

¹⁴Department of Physics, Faculty of Science, University of Zagreb, Croatia

¹⁵University of York, United Kingdom

¹⁶Istituto Nazionale di Fisica Nucleare, Perugia, Italy

¹⁷Dipartimento di Fisica e Geologia, Università di Perugia, Italy

¹⁸University of Santiago de Compostela, Spain

¹⁹Universitat Politècnica de Catalunya, Spain

²⁰Universidad de Sevilla, Spain

²¹Istituto Nazionale di Astrofisica - Osservatorio Astronomico d'Abruzzo, Italy

²²Dipartimento di Fisica, Università degli Studi di Bari, Italy

²³National Technical University of Athens, Greece

²⁴School of Physics and Astronomy, University of Edinburgh, United Kingdom

²⁵Paul Scherrer Institut (PSI), Villigen, Switzerland

²⁶Physikalisch-Technische Bundesanstalt (PTB), Bundesallee 100, 38116 Braunschweig, Germany

²⁷University of Ioannina, Greece

²⁸Instituto Superior Técnico, Lisbon, Portugal

²⁹Joint Institute for Nuclear Research (JINR), Dubna, Russia

³⁰Goethe University Frankfurt, Germany

³¹European Commission, Joint Research Centre, Geel, Retieseweg 111, B-2440 Geel, Belgium

³²Helmholtz-Zentrum Dresden-Rossendorf, Germany

³³Karlsruhe Institute of Technology, Campus North, IKP, 76021 Karlsruhe, Germany

³⁴Japan Atomic Energy Agency (JAEA), Tokai-mura, Japan

³⁵Charles University, Prague, Czech Republic

³⁶Istituto Nazionale di Fisica Nucleare, Sezione di Bologna, Italy

³⁷Dipartimento di Fisica e Astronomia, Università di Bologna, Italy

³⁸Istituto Nazionale di Fisica Nucleare, Sezione di Legnaro, Italy

³⁹Consiglio Nazionale delle Ricerche, Bari, Italy

⁴⁰Agenzia nazionale per le nuove tecnologie, l'energia e lo sviluppo economico sostenibile (ENEA), Bologna, Italy

⁴¹Istituto Nazionale di Fisica Nazionale, Trieste, Italy

⁴²Horia Hulubei National Institute of Physics and Nuclear Engineering (IFIN-HH), Bucharest

⁴³University of Granada, Spain

⁴⁴University of Vienna, Faculty of Physics, Vienna, Austria

⁴⁵Bhabha Atomic Research Centre (BARC), India

⁴⁶Gran Sasso Science Institute (GSSI), L'Aquila, Italy

⁴⁷Australian National University, Canberra, Australia

Abstract. The neutron-induced fission cross section of ^{235}U , a standard at thermal energy and between 0.15 MeV and 200 MeV, plays a crucial role in nuclear technology applications. The long-standing need of improving cross section data above 20 MeV and the lack of experimental data above 200 MeV motivated a new experimental campaign at the n_TOF facility at CERN. The measurement has been performed in 2018 at the experimental area 1 (EAR1), located at 185 m from the neutron-producing target (the experiment is presented by A. Manna et al. in a contribution to this conference). The $^{235}\text{U}(n,f)$ cross section from 20 MeV up to about 1 GeV has been measured relative to the $^1\text{H}(n,n)^1\text{H}$ reaction, which is considered the primary reference in this energy region. The neutron flux impinging on the ^{235}U sample (a key quantity for determining the fission events) has been obtained by detecting recoil protons originating from n-p scattering in a C_2H_4 sample. Two Proton Recoil Telescopes (PRT), consisting of several layers of solid-state detectors and fast plastic scintillators, have been located at proton scattering angles of 25.07° and 20.32° , out of the neutron beam. The PRTs exploit the $\Delta E-E$ technique for particle identification, a basic requirement for the rejection of charged particles from neutron-induced reactions in carbon. Extensive Monte Carlo simulations were performed to characterize proton transport through the different slabs of silicon and scintillation detectors, to optimize the experimental set-up and to deduce the efficiency of the whole PRT detector. In this work we compare measured data collected with the PRTs with a full Monte Carlo simulation based on the Geant-4 toolkit.

1 Introduction

The $^{235}\text{U}(n,f)$ cross section is considered as standard at thermal neutron energy and between 0.15 MeV and 200 MeV [1]. Its importance in nuclear reactor applications is overwhelming and, typically, it is employed as a reference in fission cross section measurements, see Ref. [2] among the others. Despite its widespread use in many fields, only two measurements are available between 20 and 200 MeV [3, 4], and no experimental points exist for neutron-induced fission cross sections above 200 MeV. At the neutron time-of-flight facility n_TOF [5], via an INFN-PTB (Istituto Nazionale di Fisica Nucleare, Physikalisch-Technische Bundesanstalt) joint experimental campaign, the $^{235}\text{U}(n,f)$ cross section from 20 MeV up to about 1 GeV has been measured relative to the $^1\text{H}(n,n)^1\text{H}$ reaction [6]. Fission events from several ^{235}U samples have been detected using fission chambers and a set of parallel plate avalanche counters (PPAC) [6]. To measure n-p scattering in presence of an intense γ flash and a continuous neutron energy distribution, three Proton Recoil Telescopes (PRTs) were specifically designed. Since fission fragments and recoil protons have been measured by different experimental set-ups, efficiencies must be precisely known and a fully characterization of the detectors is mandatory. Here, we present the model used to simulate the PRT systems employing the GEANT4 toolkit [7]. Some preliminary results and comparisons to experimental data for the two of the three PRT detectors of INFN conception are also shown.

*e-mail: nicholas.terranova@enea.it

2 Detection system overview

To measure n-p scattering, three PRT detection systems were placed in front of Polyethylene targets as shown in figure 1. In order to cover a broader neutron energy do-

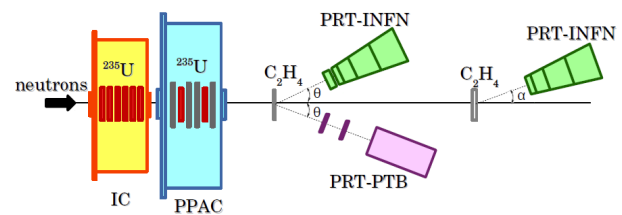


Figure 1. Experimental set-up for the $^{235}\text{U}(n,f)$ cross section relative to $^1\text{H}(n,n)^1\text{H}$.

main, the design proposed in Ref. [8] was extended to multi-stage systems with increased particle discrimination potential. Two INFN-PRTs consisting of several layers of solid-state detectors and fast plastic scintillators were designed to cover the whole neutron energy range from 20 MeV to 1 GeV. The former PRT, called hereinafter INFN-PRT-L, was foreseen for lower energies (from 20 to about 200 MeV), being equipped with two frontal solid-state layers preceding 4 stages of plastic scintillation material. The latter (INFN-PRT-H) is made only of multiple scintillation stages, since thin solid-state layers would not contribute to any detection at higher energies. Both were located in front of Polyethylene targets of different thicknesses,

at proton scattering angles of 25.07° and 20.32° , respectively, out of the neutron beam. The ΔE -E technique has been used to perform particle identification and subtract the background both from secondaries produced by reactions on Carbon nuclei in the Polyethylene target, and from spurious energy deposits due to undesired particles hitting the detector sensitive material.

3 Monte Carlo simulation development

The evaluation of the n-p scattering obtained by Arndt and his collaborators [9, 10] was accepted by the NE-ANDC/INDC as a primary standard for cross section measurements in the 20-350 MeV range [11]. In Geant4, the application developer is called to directly define the physics of his own problem adopting the physical models made available in the toolkit. To obviate such a complexity, reference physics list classes are already defined by Geant4 developers to be easily included by users for implementing new applications. Unfortunately, no reference physics list involves Arndt data. In figure 2 several

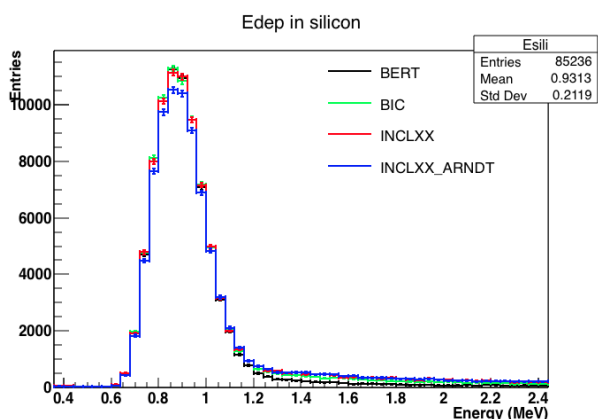


Figure 2. Comparison between different physics lists in Geant4 for energy deposition in the first solid-state layer of the PRT detector for 50 MeV neutrons impinging on the target.

reference physics lists which are available in Geant4 have been compared to a user-defined physics class including Arndt evaluation. A simplified ΔE -E detector made of one solid-state layer coupled to a plastic scintillator was chosen to perform nuclear data investigations. The energy deposited in the silicon layer is lower than what is obtained using reference physics lists (labeled with the specific intra-nuclear cascade model chosen in these pre-defined classes). The choice of Bertini, BIC (Binary Cascade) or the INCL (Intra-Nuclear Cascade of Liege) does not really impact the energy peak height. The phase-shift solution, at the basis of the Arndt evaluation, provides, instead, some significant discrepancies if used in place of the hadronic elastic model of the CHIPS (CHiral Invariant Phase Space) package used in Geant4 reference physics lists. Investigations on the most suitable physical models as functions of the incident neutron energy over the whole 20 MeV-1 GeV domain is ongoing.

A detailed Monte Carlo model of the INFN-PRTs including the reference Arndt data for the only n-p scattering was developed using the Geant4 toolkit [7]. The low statistics (only 25000 entries in coincidence for the first and the second scintillator over 10^9 neutrons simulated) made the computation quite time consuming (about 2 days on a conventional PC in single thread for 10^9 neutrons). Parallel single thread simulations were dispatched on multiple cores to improve statistics and reduce the computing time. Independent seeds were generated using the C++11 `std::seed_seq` to initialize the Ranecu random number generator in Geant4. Figure 3 shows a scatter plot of 512 sim-

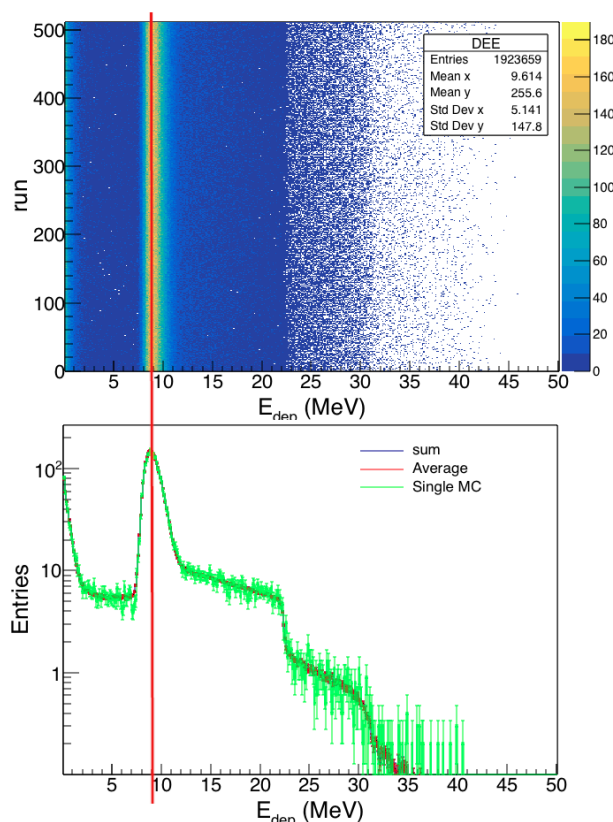


Figure 3. Scatter plot of the energy deposition in the first scintillator of the INFN-PRT-L (top). The batch average of 512 10^8 -neutrons simulations is compared to a single 10^9 -neutrons simulation (bottom).

ulations giving the energy deposited in the first scintillator of the INFN-PRT-L detector. 10^8 neutrons at 50 MeV were simulated as primary particles for each run, sampled from a $0.6\text{-}\sigma$ -Gaussian spatial distribution. Batch averages and standard deviations were calculated showing a perfect agreement with a single 10^9 -neutrons simulation (whose uncertainties were estimated supposing a Poisson distribution). This approach allowed us to perform multiple single-thread stable calculations and rigorous means to quantify uncertainties to be propagated during the particle identification process. Variance reduction techniques are foreseen and their implementation is ongoing.

4 Conclusions and Results

A Polyethylene (C_2H_4) target was used to maximize the Hydrogen content in a solid target to detect recoil protons from the $^1H(n,n)^1H$ reaction. In order to extract flux information, a set of measurements, in the original geometrical configuration in figure 1, with Carbon samples of equivalent thicknesses facing the neutron beam, were performed during the experimental campaign.

Using a simplified ΔE -E detector, the impact of undesired contributions coming from Carbon nuclei in a Polyethylene sample was estimated using Geant4. 10^9 neutrons at

Ref. Physics List	Any particle	Protons	Deuterons
Polyethylene			
BERT	76700 ± 300	76200 ± 300	450 ± 20
BIC	82600 ± 300	82100 ± 300	430 ± 20
INCLXX	85800 ± 300	83600 ± 300	1970 ± 40
Carbon			
BERT	6790 ± 80	6120 ± 80	610 ± 30
BIC	13700 ± 100	13100 ± 100	530 ± 20
INCLXX	17600 ± 100	14900 ± 100	2500 ± 50
Hydrogen			
BERT	71583 ± 300	71566 ± 300	2 ± 1
BIC	71582 ± 300	71538 ± 300	19 ± 4
INCLXX	71600 ± 300	71581 ± 300	6 ± 3

Table 1. Monte Carlo entries in coincidence for a simplified ΔE -E detector, using targets of different materials and several physics lists in Geant4. Pure Carbon and Hydrogen targets are made of fictitious materials having nuclei densities which correspond to those in the Polyethylene target.

50MeV impinging on pure Hydrogen and Carbon fictitious samples were simulated using different reference physics lists in Geant4. Nuclei densities were assumed identical to those contained in the Polyethylene target. Table 1 shows how the events in coincidence in the two layers of a simplified ΔE -E detector are systematically lower than the sum of the events obtained using pure Hydrogen and Carbon, exhibiting self-shielding and attenuation effects. Extensive Monte Carlo simulations have been performed to characterize the INFN-PRT-L and the INFN-PRT-H telescopes. A notable discrimination capability given by the multiple segmentation of the detectors has been preliminarily demonstrated for different neutron energies. Collecting signals in coincidence between several multiple layers allows, in fact, to easily recognize different secondary particles coming from inelastic reactions on Carbon. A fully characterization of the detectors in terms of detection limits, expected punch through energies, intrinsic and global efficiency is ongoing.

Background calculations were performed both to estimate the contributions to the INFN-PRT-L of backscattered secondary particles coming from the target in front of the INFN-PRT-H telescope, and to investigate if particles coming from the former thinner sample may deposit significant energy in the farthest telescope. No significant contributions were observed for both the scenarios.

A thorough comparison between experimental data and Monte Carlo simulations is under achievement. A preliminary result showing Monte Carlo calculations and cali-

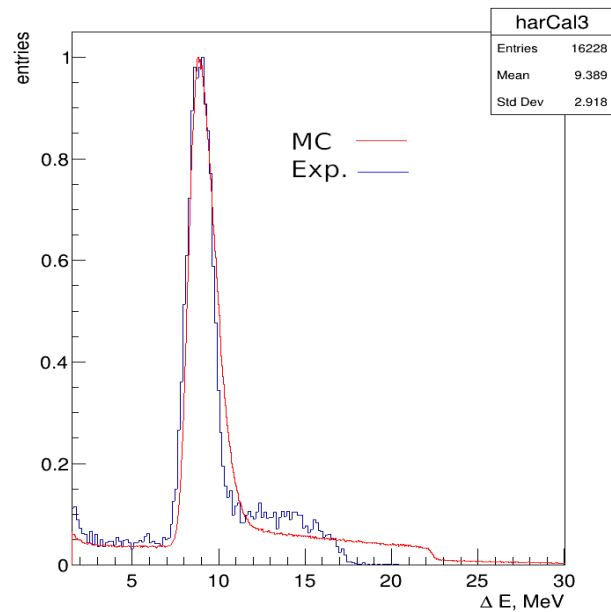


Figure 4. Monte Carlo and experimental data comparison for the energy deposition in the first scintillator of the INFN-PRT-L detector (for 50 MeV neutrons impinging on the target).

brated experimental data for the energy deposited in the first scintillator of the INFN-PRT-L and for 50 MeV neutrons impinging on the target is given in figure 4. Discrepancies can be observed for energies above 11 MeV. These may be presumably attributed to deuteron energy depositions coming from reactions on Carbon, which may not be correctly simulated in Geant4 using the available physics lists.

Acknowledgments

The authors wish to thank the National Center of the INFN for Research and Development in Information and Communication Technologies (CNAF) for their computational support.

References

- [1] A.D. Carlson et al., Nuclear Data Sheets **148**, 143 (2018)
- [2] Tarrío et al., Physical Review C **83**, 044620 (2011)
- [3] A.D. Carlson et al., International Conference on Nuclear Data for Science and Technology p. 518 (1991)
- [4] R. Nolte et al., Nuclear Science and Engineering **156**, 197 (2007)
- [5] C. Guerrero et al., European Physical Journal A **49**, 27 (2013)
- [6] A. Manna et al., International Conference on Nuclear Data for Science and Technology (2019), to be published
- [7] S. Agostinelli et al., Nuclear Instruments and Methods in Physics Research Section A: Accelerators, Spectrometers, Detectors and Associated Equipment **506**, 250 (2003)

- [8] V. Dangendorf et al., Nuclear Instrumentation Methods A **469**, 205 (2001)
- [9] R.A. Arndt et al., Physical Review D **35**, 128 (1987)
- [10] R.A. Arndt et al., Physical Review C **50**, 2731 (1994)
- [11] IAEA, *International evaluation of neutron cross-section standards* (2007)